Available online at www.sciencedirect.com
ScienceDirect
Journal of Magnetic Resonance 190 (2008) 95–104
JMR Journal of Magnetic Resonance
www.elsevier.com/locate/jmr

# A closer look into DESIRE for NMR microscopy

Markus Weiger *, Yi Zeng, Michael Fey

*Bruker Biospin AG, Industriestrasse 26, CH-8117 Faellanden, Switzerland*

Received 16 July 2007; revised 2 October 2007
Available online 12 October 2007

**Abstract**

The major challenge of nuclear magnetic resonance (NMR) microscopy at a spatial resolution of a few micrometers is to obtain a sufficiently high signal-to-noise-ratio (SNR) within a reasonable measurement time. As a particular difficulty, molecular self-diffusion poses a serious limitation to true spatial resolution and SNR if conventional Fourier encoding techniques are used. Opposed to that, the alternative DESIRE (Diffusion Enhancement of SIgnal and REsolution) approach to NMR microscopy utilises diffusion to increase the SNR. Being a real-space imaging method, spatial localisation is accomplished by saturation pulses while diffusion continuously replaces the saturated by unsaturated spins. For this technique a signal enhancement of up to three orders of magnitude has been predicted and initial experimental data have provided a proof of principle. In the present work, a detailed investigation of one-dimensional (1D) DESIRE is presented including simulations of a real implementation of the method, a quantitative experimental analysis, and basic 1D imaging. The simulations reveal the importance and provide the means of ensuring the true spatial resolution for this particular way of localisation, enable the selection of useful experimental parameters, and predict the specific image contrast to be expected around barriers restricting diffusion. Experimental data are presented with resolutions down to 3 μm and DESIRE enhancement up to 25 that are in good agreement with the simulation results. In particular, 1D DESIRE imaging in a phantom confirms the expected signal drop close to barriers due to spatially restricted diffusion.


*Keywords:* NMR microscopy; DESIRE; Diffusion; Spatial resolution; Signal enhancement

## 1. Introduction

Nuclear magnetic resonance (NMR) microscopy has the great potential of providing the plurality of NMR contrast mechanisms also to very small biological samples, such as e.g. single cells [1]. However, at a spatial resolution of a few micrometers it is increasingly difficult to obtain a sufficiently high signal-to-noise-ratio (SNR) within a reasonable measurement time. Furthermore, conventional Fourier encoding techniques suffer from a loss of true resolution due to a filtering effect in *k*-space arising from molecular self-diffusion [2]. This effect can be reduced by the use of very strong field gradients. However, for frequency-encoding this leads to a further decrease in SNR, favouring purely phase-encoded methods [3]. In this context high magnetic fields and dedicated gradient and radio-frequency (RF) coils enable to considerably push the spatial resolution [4]. However, the SNR achievable per unit time remains the limiting factor in NMR microscopy.

Instead of suffering from diffusion, the DESIRE technique (Diffusion Enhancement of SIgnal and REsolution) [5] follows the completely different approach of utilising the effects of diffusion for enhancing the SNR. As opposed to conventional NMR imaging DESIRE is a real-space approach where spatial localisation is not accomplished by means of Fourier encoding but with spatially selective saturation of the volume of interest. The saturation is followed by RF excitation and acquisition, and the obtained data provides the contrast information for the chosen voxel by subtraction from a reference signal acquired without saturation. With this type of imaging, signal enhancement is achieved by using an extended saturation period during

* Corresponding author. Fax: +41 44 825 96 38.
*E-mail address:* markus.weiger@bruker-biospin.ch (M. Weiger).

1090-7807/$ - see front matter © 2007 Elsevier Inc. All rights reserved.
doi:10.1016/j.jmr.2007.10.003

that fresh spins diffuse into the directly saturated volume while saturated spins move away from it. This way a much larger volume of saturated spins will represent the selected voxel, corresponding to an enhanced signal difference. In their original work [5] the authors presented one-dimensional (1D) images acquired with the described method, demonstrating a signal enhancement that increased with the duration of the saturation period.

The prospects of DESIRE for NMR microscopy were assessed theoretically by Pennington who predicted possible signal enhancements of one to three orders of magnitude, depending on diffusion, resolution, and the number of resolved spatial dimensions [6]. Using a specific implementation of 1D DESIRE Ciobanu et al. [7] experimentally observed an enhancement in the expected range for a saturation thickness of 8 μm. The goal of the present work is to further investigate the usefulness of DESIRE for NMR microscopy by gaining deeper insight into the mechanisms of the technique. For simplicity but without loss of generality the 1D case was selected to elucidate several aspects such as signal enhancement, spatial resolution, and contrast by means of simulations and experiments. In particular, the important role of the various parameters of the saturation period and the image contrast close to barriers are demonstrated. Experimental data are presented with resolutions down to 3 μm and DESIRE enhancement up to 25, including the first DESIRE image actually resolving structural features.

## 2. Theory

### 2.1. DESIRE enhancement

For the DESIRE technique spatial localisation is accomplished by spatially selective saturation of the magnetisation using RF and gradient pulses. The image value for the chosen voxel is obtained by taking the difference of the reference and the partly saturated signal. Neglecting relaxation effects during data acquisition this difference is given by the saturated volume

$$V = \int_r S(r)\,\mathrm{d}r, \tag{1}$$

where $S(r) = 1 - M_z(r)$ is the 1D spatial saturation profile with the distance $r$ from the voxel centre, the longitudinal magnetisation $M_z(r)$, and normalised equilibrium magnetisation $M_0 = 1$. The fractional amount of enhanced signal $E$ for DESIRE as defined in Ref. [6] is then expressed with the directly saturated volume $V_0$ and that after completed DESIRE saturation $V_D$ by

$$E = \frac{V_D}{V_0} - 1. \tag{2}$$

The idealised situation assumed in Ref. [6] is a source of continuously saturated spins of spatially rectangular shape of width $d$, employed for a duration $T$. Here, the DESIRE saturation profile outside the directly saturated region can be expressed analytically with the error function

$$S(r) = 1 - \mathrm{erf}\left(\frac{|r - d/2|}{\sqrt{4TD}}\right), \tag{3}$$

where $D$ is the coefficient for self-diffusion. Hence, for certain values of $T$ and $D$ and different resolution $d$ the profile shape is only shifted, the gained saturation volume

$$\Delta V = \int_{r=-\infty}^{\infty} \left(1 - \mathrm{erf}\left(|r|/\sqrt{4TD}\right)\right) \mathrm{d}r \tag{4}$$

is constant, and the enhancement is

$$E = \Delta V / d. \tag{5}$$

A possible real implementation of a DESIRE preparation as proposed in Ref. [7] and shown in Fig. 1 is a series of $n$ saturation pulses of duration $t_p$ repeated after $t_d$. The associated development of the magnetisation under diffusion can be calculated numerically using the Bloch–Torrey equations [8], thus enabling to determine the expected saturation profile, saturated volume, and DESIRE enhancement.

### 2.2. Spatial resolution

Real RF pulses of limited duration create saturation profiles that deviate from the ideal rectangular shape.

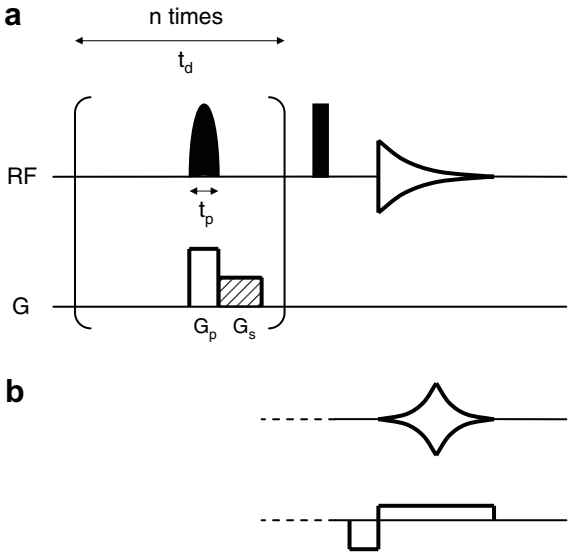


Fig. 1. Schemes of DESIRE experiments. The DESIRE preparation depicted in (a) consists of a series of $n$ saturation pulses repeated after $t_d$, thus resulting in a total saturation duration $T = nt_d$. The spatial resolution achieved by selective excitation of duration $t_p$ is determined by the bandwidth of the RF pulse and the gradient strength $G_p$ according to Eq. (6). Spoiling of the created transverse magnetisation is accomplished by a gradient of strength $G_s$, applied preferably in a different direction than $G_p$. In (a) the preparation is followed by the acquisition of a free induction decay representing the remaining longitudinal magnetisation. The sequence shown in (b) serves to map the saturated profiles. While employing the identical saturation scheme as in (a) a gradient echo method is used afterwards. For both schemes a reference signal is acquired without DESIRE preparation.

Therefore, a useful description of spatial resolution is required. A common definition of the latter is the full width at half maximum (FWHM) of the image point spread function (PSF). For the case of DESIRE the PSF is given by the saturation profile. Hence, the spatial resolution can be calculated according to

$$d_{\mathrm{FWHM}} = \frac{\mathrm{bwfac}}{t_{\mathrm{p}}\gamma G_{\mathrm{p}}}, \tag{6}$$

where bwfac is the bandwidth factor characteristic for a certain RF pulse, $\gamma$ is the gyromagnetic ratio of the excited nucleus, and $G_{\mathrm{p}}$ is the strength of the constant gradient applied during the RF pulse.

An alternative or complementing definition of spatial resolution considers more the shape and side lobes of the saturation profile. The spatial resolution $d_{\mathrm{vol}}$ is identical to the range within that a given fraction volfrac of the PSF must be contained

$$\int_{-d_{\mathrm{vol}}/2}^{d_{\mathrm{vol}}/2} \mathrm{PSF}(r)\,\mathrm{d}r = \mathrm{volfrac}\int_{-\infty}^{\infty} \mathrm{PSF}(r)\,\mathrm{d}r. \tag{7}$$

For Fourier imaging volfrac = 0.875 leads to $d_{\mathrm{vol}}$ being the nominal resolution $d$, i.e. the distance of two side lobes of the sinc-shaped PSF, whereas $d_{\mathrm{FWMH}} = 1.21d$. In contrast to that, for real-space saturation techniques the volume definition leads to the larger resolution values. Here, the PSF cannot have negative values that partly cancel out the integral of side lobes as it occurs in the Fourier case

For a single, short saturation pulse applied at equilibrium magnetisation the magnetisation just after the pulse provides the saturation profile that determines the resolution. However, for a series of short pulses the situation is more complicated because the saturation may be applied to pre-saturated locations. Therefore, an effective profile $S_{\mathrm{eff}}(r)$ is introduced that takes into account the relative amount of magnetisation saturated at each location. It is defined as the cumulated differences of the longitudinal magnetisation $M_{z,i}^{-}(r)$ before and $M_{z,i}^{+}(r)$ after the $i$th pulse

$$S_{\mathrm{eff}}(r) = \sum_{i=1}^{n}\left(M_{z,i}^{-}(r) - M_{z,i}^{+}(r)\right). \tag{8}$$

From the effective profile the associated effective resolution values $d_{\mathrm{eff}}$ can be calculated in the same way as for the single pulse profile. Furthermore, an effective DESIRE saturation volume is defined penalising a signal increase that comes at the cost of reduced spatial resolution

$$V_{\mathrm{D,eff}} = V_{\mathrm{D}}\frac{d_0}{d_{\mathrm{eff}}}, \tag{9}$$

where $d_0$ is a resolution value derived from the single pulse profile. The corresponding effective enhancement $E_{\mathrm{eff}}$ is then calculated according to Eq. (2).

If the pulse duration is not short compared to $d^2/D$ diffusion during the pulse has to be considered in order to obtain the effective profile. In this case each pulse can be calculated by integration of the Bloch–Torrey equations using $m$ sufficiently short time intervals. This changes Eq. (8) to

$$S_{\mathrm{eff}}(r) = \sum_{i=1}^{n}\sum_{j=1}^{m}\left(M_{z,i,j}^{-}(r) - M_{z,i,j}^{+}(r)\right), \tag{10}$$

where $M_{z,i,j}^{-}(r)$ and $M_{z,i,j}^{+}(r)$ represent the magnetisation before and after RF application for the $j$th interval of the $i$th pulse.

### 2.3. SNR

In order to provide an upper limit for the SNR gain of DESIRE as compared with Fourier imaging it is assumed that for DESIRE the full available sample volume of size $L$ is saturated, resulting in an SNR advantage of $L/d$. Here, $L$ and $d$ describe volumes of arbitrary dimensionality. On the other hand, with Fourier imaging $N = L/d$ samples are acquired, leading to an SNR factor of $\sqrt{N}$. For the latter case, a purely phase-encoded method is assumed, hence the bandwidth can be chosen identically in both methods. In total, the SNR gain of DESIRE would be $\sqrt{N}$ which is proportional to $1/\sqrt{d}$ for constant $L$. For example, for 3D imaging with $N = 64^3$, the maximum SNR gain would be $8^3$, and the associated time saving $8^6$. However, in closed compartments the volume that can be saturated is restricted, limiting the maximum possible signal enhancement and the SNR.

## 3. Methods

### 3.1. Simulations

Starting from equilibrium magnetisation the development of the magnetisation vectors in a 1D spatial range was simulated for a DESIRE preparation consisting of a series of pulses as depicted in Fig. 1a. The calculation was carried out by discrete numerical integration of the Bloch equations generalised for diffusion by Torrey (Eqs. (1–3) in Ref. [8]). For improved efficiency, RF pulses were treated as rotations (see e.g. Eq. 4.2.25 in Ref. [9]) either in one or in multiple pieces in case of diffusion. The spatial range was set to a suitable value between 500 and 2000 μm. The sizes of the time and spatial intervals were adapted automatically according to the values of $d$, $D$, $t_{\mathrm{d}}$, $t_{\mathrm{p}}$, and of the spatial range. For the saturation, block and sinc-shaped pulses were used, the latter employing only the main temporal lobe. The respective values of bwfac of the pulses are 0.86 and 1.24. Gradient spoiling after the RF pulses was accomplished by setting the transverse magnetisation components to zero. If relaxation was taken into account, the constants $T_1$ for longitudinal and $T_2$ for transverse relaxation were assumed to be identical. For determination of $d_{\mathrm{vol}}$ volfrac = 0.875 was used. Calculation of diffusion restricted by impermeable barriers was carried out by using the boundary condition for reflection with the

spatial derivative of the magnetisation set to 0 at the location of the barrier. See also Eq. (3) in Ref. [10] or Eq. (8) in Ref. [11]. The simulation was implemented in Matlab and executed on a standard PC, with the calculation times per saturation procedure ranging between several seconds and minutes.

### 3.2. Experiments

Experiments were conducted at 7 T using a Bruker standard bore magnet operated with an AVII spectrometer and equipped with a MIC5 standard microimaging probe. With the maximum current of 60 A provided by the GREAT gradient amplifier the largest possible gradient strength was 2.88 T/m. A sample tube of 5 mm diameter was filled with pure water and held at a constant temperature of 292 K. The constants $T_1 = 2.6$ s and $D = 2.3\ \mu m^2/ms$ were determined with the corresponding standard methods. Gradient amplifier offsets and eddy current compensation were carefully adjusted in order to minimise systematic errors. DESIRE experiments as depicted in Fig. 1a were performed with the saturated slice being perpendicular to the sample axis, $n = 5$–$500$ saturation pulses of durations $t_p = 3$ or 5 ms and spacing $t_d = 20$ or 33 ms, slice selection gradients $G_p$ up to 2.43 T/m, a spoiling gradient of strength $G_s = 0.58$ T/m and duration 2 ms applied in plane, a 30° hard pulse of duration 50 μs for excitation, a repetition time of 30 s, a data acquisition time of 2.5 s, BW = 10 kHz, and 16 averages. The free induction decay data was Fourier transformed and phase and baseline corrected. The signal value was calculated by integration of the real part of the spectrum over 30% of the spectral range, corresponding to an actual bandwidth of 3 kHz. Profile imaging with the sequence shown in Fig. 1b was performed with a spatial resolution of 10 μm in a field of view of 3 cm, an acquisition time of 1.25 ms, an echo time of 1.13 ms, and 16 averages.

## 4. Results

### 4.1. Simulations

The simulations of the saturation profiles serve to better understand the mechanisms of DESIRE saturation. Moreover, for real experimental situations suitable parameter settings can be found for pulse shape, $n$, $T$, and $t_p$ depending on $d$, $D$, and $T_1$.

Fig. 2 shows magnetisation profiles demonstrating the influence of the different parameters. Without diffusion, the side lobes present already after a single block pulse are greatly enhanced in the DESIRE profile as well as in the identical effective profile (Fig. 2a). Hence, a signal enhancement is obtained which is not due to diffusion but to repetitive saturation. As the signal gained in this way originates mainly from locations away from the main lobe the localisation is lost to a great extent. The block pulse with diffusion (Fig. 2b) achieves a clearly improved but still unfavourable localisation as shown by the effective profile. Opposed to that the spatial definition obtained with the sinc-shaped saturation (Fig. 2c) is much more confined to the main lobe due to the very small side lobes created by this pulse. As demonstrated in Fig. 2d the situation is even more improved when going to smaller $d$, which is the actual idea of applying the DESIRE technique.

Nevertheless, the shape and width of the main lobe vary with $D$, indicating a general, method-inherent diffusion-dependence of the spatial resolution of DESIRE. Fig. 3 (top) shows this behaviour of the FWHM and volume resolution for a wide range of $D$. Generally, the resolution is better for higher diffusion due an increased degree of replaced saturated spins. For extremely large diffusion the effective profile would approach that of the single pulse, thus actually providing the nominal resolution. The heavy side lobes of the block pulse are penalised in the volume resolution which is about an order of magnitude larger than for the sinc pulse. Note that steps in the curves indicate the volume range border passing locations with changes of the second derivative. Fig. 3 (bottom) demonstrates the difference between apparent and truly useful DESIRE enhancement. For the block pulse the comparison of the DESIRE saturated volume with that of the single pulse pretends large $E$ even with low diffusion. This is corrected by using $E_{eff}$, in particular with the weighting by the volume resolution. Also for the sinc pulse the values of $E_{eff}$ are reduced with respect to $E$, however, to a much lower extent.

Very similar results would be obtained for constant $D$ and decreasing values of $d$, thus making the aspect of reduced effective resolution less critical at very high nominal resolution. However, although the setup in Fig. 2d shows very good resolution properties the saturation efficiency and hence the enhancement are below that given for the ideal case. As shown in Fig. 2e this compromise can be shifted towards higher efficiency at the price of reduced resolution by using more pulses at constant saturation duration. Obviously, longer diffusion delays allow for better replacement of saturated spins and hence better resolution, but more pulses increase the final saturated volume. Fig. 4 shows that the two competing effects lead to optimum values $n_{opt}$ for the different $E_{eff}$. Investigating this dependence for other values of $d$ yields that $n_{opt}$ increases for smaller $d$.

Finally, Fig. 2f shows an example of a non-instant, extended pulse using the relatively extreme situation of a quasi-continuous excitation with $n = 10$ sinc pulses of $t_p = 100$ ms duration. Looking at the effective profile it is remarkable that the spatial resolution suffers only slightly due to the long pulses, which is in strong contrast to the assumptions made in Ref. [6] in order to determine gradient hardware requirements. However, some reduction of the saturated volume has to be accepted for long pulses.

So far, relaxation has been neglected. Setting $T_1$ to a finite value yields the not unexpected result that for increasing saturation duration $T$ the enhancement values approach an asymptotic value and cannot be further

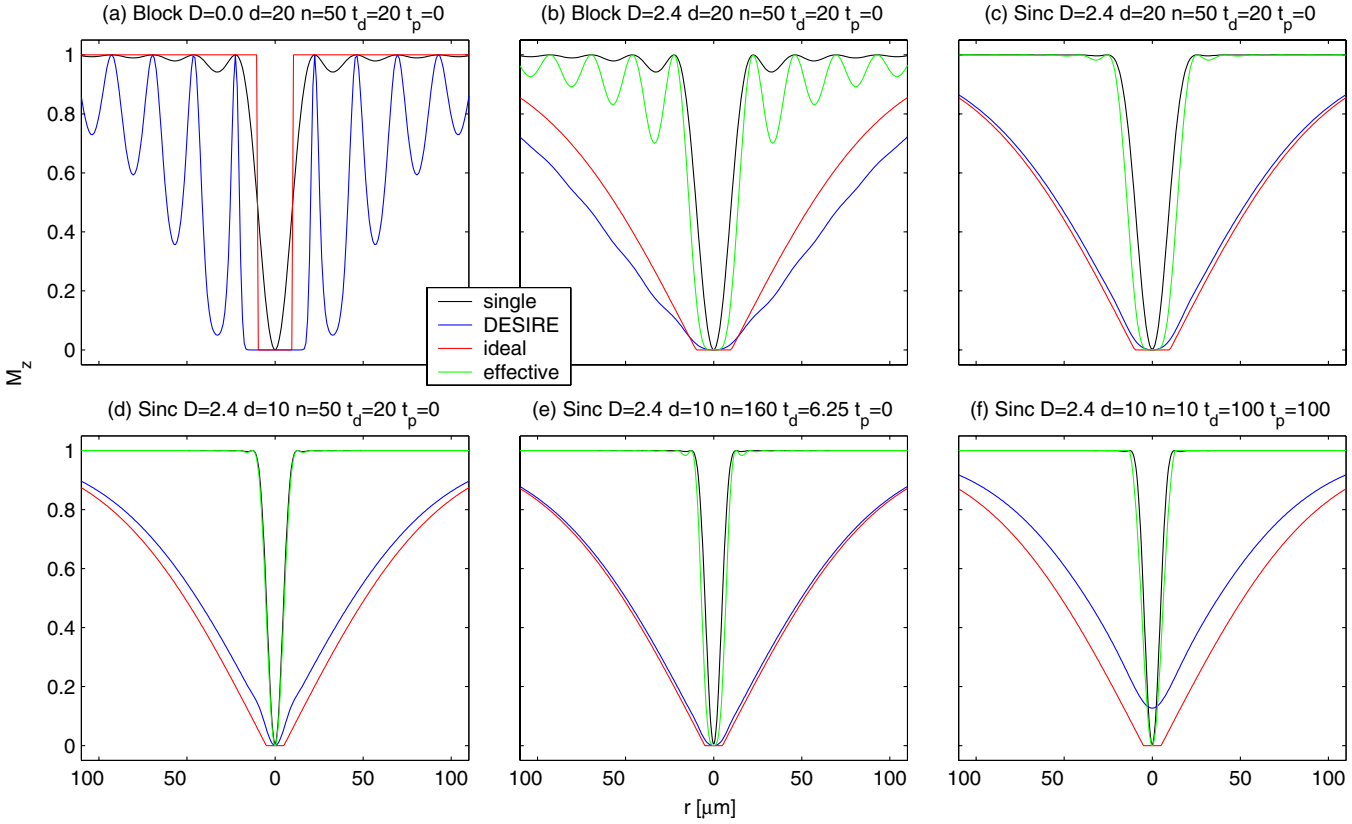


Fig. 2. Simulated magnetisation profiles for DESIRE preparation at different diffusion constants $D$ (µm$^2$/ms) and with different parameters $d$ (µm), $n$, $t_d$ (ms), $t_p$ (ms), a saturation period $T = 1$ s and $T_1 = \infty$. The graphs show the profiles after a single pulse (black), after completed DESIRE saturation (blue), for the ideal setup from Ref. [6] (red), and the effective profile revealing the true resolution (green). Note that in order to allow for a useful comparison the effective profiles are scaled in a way to have a minimum value of 0. (a) The block pulse without diffusion shows an apparent enhancement due to the side lobes being increased by repetitive saturation. (b) This effect is reduced with diffusion but still strongly affects the effective resolution. (c) Opposed to that the sinc pulse only shows an increased width of the main lobe. (d) For smaller $d$ the effective resolution is further improved. (e) Using more pulses gives increased enhancement but a wider main lobe of the effective profile. (f) Surprisingly, even very long pulses still provide good effective resolution. See Figs. 3 and 4 for the effective resolution and DESIRE enhancement for large ranges of $D$ and $n$, respectively, as derived from the simulated effective profiles.

improved by increasing the saturation duration beyond $3T_1$. The spatial resolution is essentially independent of $T$.

In summary of the first part of the simulations some important conclusions can be drawn. Avoiding pulse shapes that create considerable side lobes in the longitudinal magnetisation is essential to maintain the spatial resolution of DESIRE. A reasonable choice is the proposed sinc pulse which is also relatively time efficient in generating a certain bandwidth. Furthermore, for given $d$, $D$, and $T_1$, values of $n$ and $T$ can be derived that provide a good compromise between enhancement and resolution. However, generally the latter is a function of $D$. Somewhat surprisingly, $t_p$ is not a critical parameter.

The second part of the simulations concerns DESIRE imaging in objects where diffusion is restricted by impermeable barriers. Fig. 5 shows profiles obtained for saturations applied in the vicinity of the barrier located at $z = 0$. For the profiles on the left shown with bold lines it was assumed that magnetisation is excited only on this side of the barrier. Essentially this means that the barrier has at least the width of the pulse. The asymmetric shapes of the profiles indicate how the diffusing molecules are reflected by the barrier. For the profiles drawn with dashed lines the barrier was assumed to be infinitesimally thin. This affects primarily saturations hitting the barrier to a certain degree, thus exciting magnetisation on both sides.

Based on these profiles DESIRE imaging for single-sided saturation was simulated for compartments of different size and for different $D$. Fig. 6 shows the calculated enhancement which is assumed to dominate the image contrast. The molecular diffusion in the example on the very left is only restricted on one side. As expected from the profiles the signal intensity decreases when the barrier is approached. At the position of the barrier it reaches half of the possible maximum corresponding to the solid green profile shown in Fig. 5. A similar behaviour is observed in the closed compartments with the maximum possible signal intensity and the signal shape depending on the compartment size and on $D$.

Fig. 7 shows the expected enhancement for the saturation pulse acting on both sides of a thin barrier. Close to the barrier, when the saturation pulse shape is split by the latter, the intensity suddenly peaks which corresponds

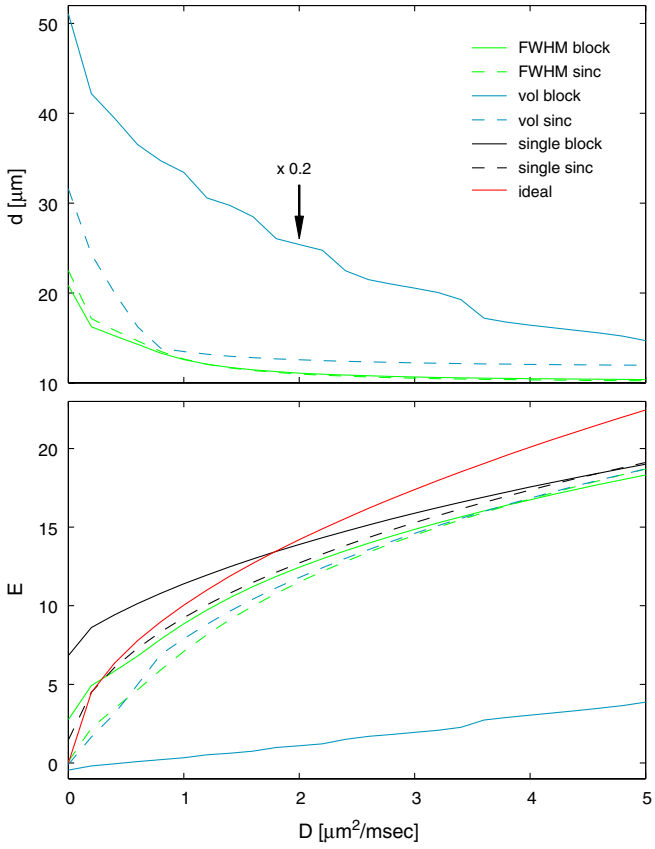


Fig. 3. Effective resolution (top) and DESIRE enhancement (bottom) as a function of the diffusion constant $D$ for block (solid lines) and sinc (dashed lines) shaped saturation pulses with parameters $d = 10$ µm, $n = 100$, $t_d = 10$ ms, $t_p = 0$, and $T_1 = \infty$. The FWHM resolution (green) of the effective saturation profiles behaves very similar for both shapes. However, the volume resolution (blue) of the block pulse is about an order of magnitude larger than that of the sinc pulse, hence penalising the increased side lobes shown in Fig. 2a and b. According to these observations, the enhancement of the block pulse calculated by comparison with the single saturation (black) strongly overestimates the useful signal gain, whereas the effective enhancement weighted with the volume resolution is even negative. All other enhancement values lie within a reasonable range around the ideal setup (red) with the signal gain generally growing for increasing $D$.

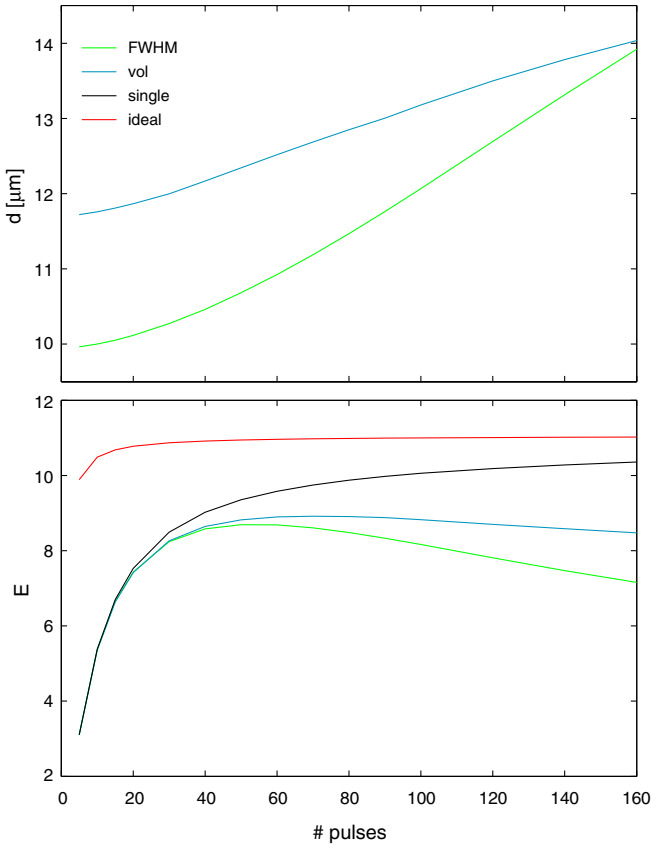


Fig. 4. Effective resolution (top) and DESIRE enhancement (bottom) as a function of the number $n$ of sinc-shaped saturation pulses with parameters $d = 10$ µm, $t_p = 0$, $T = 1$ s, $D = 2.4$ µm²/ms, and $T_1 = \infty$. Both resolution criteria show increasing values for larger $n$ as the replacement of the saturated spins is less complete. Looking at the enhancement, the values calculated for the ideal setup as well as those with the single pulse reference increase with $n$. In contrast to that the curves for the effective enhancement show maximum values at $n = 54$ for the FWHM and $n = 70$ for the volume resolution. For example profiles see Fig. 2d and e.

to the dashed profiles in Fig. 5. For this simulation the saturation was moved in steps $d/5$ to sufficiently resolve the signal transition. However, in a straightforward DESIRE imaging experiment the step-size will be set to $d$. Hence the barrier is hit at any position or even missed, resulting in any image intensity in the full range of the shown peak. Alternatively, a kind of sub-resolution could be created by actually using a step-size smaller than the saturation width, thus enabling a more accurate localisation and characterisation of the barrier.

### 4.2. Experiments

As an initial illustration, Fig. 8 shows three examples of DESIRE saturation profiles for different parameter settings with only minor differences between the measured and the simulated results. Note the slightly peculiar shape of the central profile which is composed by the already diffused saturation of the first four pulses and by the unperturbed saturation of the last one.

Coming to the real DESIRE experiments, calculation of $E$ according to Eq. (2) requires experimental determination of $V_D$ and $V_0$. The latter value is very critical as the saturation volume for small $d$ obtained from a single pulse is very small compared with the full sample volume detected in the reference experiment. Therefore, similar to the procedure suggested in Ref. [7] $V_0$ was measured for $d = 2000$, 1000, and 500 µm and extrapolated for smaller $d$ according to $V_0 = \varepsilon d$. The proportionality constant determined in this way was $\varepsilon = 6.9 \cdot 10^{-5}$ µm$^{-1}$. As $V_0$ was normalised to the reference signal without saturation the reciprocal value of $\varepsilon$ directly gives the effective visible sample length of 1.4 cm.

Fig. 9 shows $E$ as a function of $d$ where the experimental results agree reasonably well with the simulated values. Note that the step for the smallest $d = 3$ µm is due to a

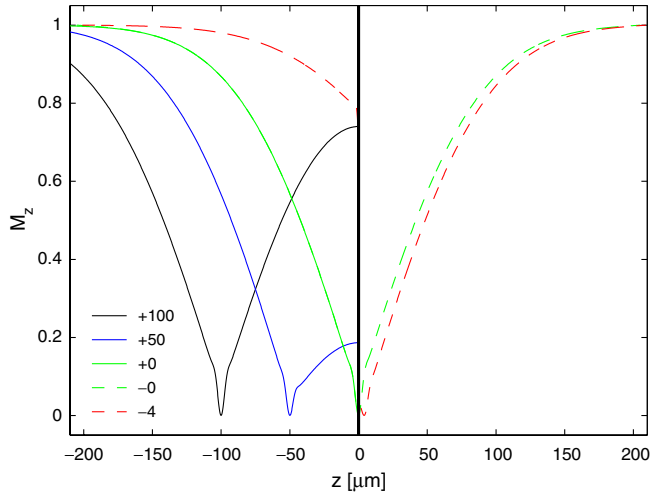


Fig. 5. Simulated magnetisation profiles showing DESIRE saturation in the vicinity of an impermeable barrier using the parameters $d = 5$ µm, $n = 100$, $t_d = 10$ ms, $t_p = 0$, $D = 2.4$ µm$^2$/ms, and $T_1 = \infty$. For the results depicted with solid lines it was assumed that magnetisation can be excited only on the left-hand side of the barrier [negative $z$ values of the saturation centre (µm)]. The dashed lines show profiles obtained for an infinitesimally thin barrier with spins saturated on both sides of the barriers (positive $z$ values). Note that the dashed green profile for $z = -0$ is continued by the solid green line on the left side.

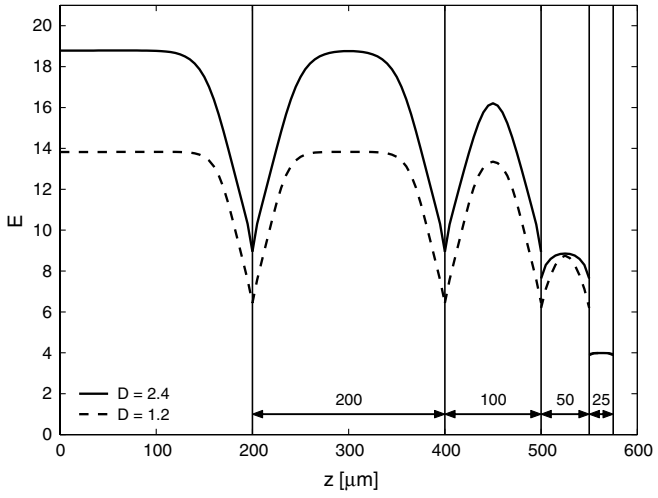


Fig. 6. Simulated DESIRE enhancement for diffusion restricted by impermeable barriers using the same saturation parameters as in Fig. 5 but for two different values of $D$ (µm$^2$/ms). In the example shown on the very left diffusion is restricted only on one side by the barrier at $z = 200$ µm. All other results show the enhancement in closed compartments with the respective size given in (µm). In all cases signal was generated only inside the compartment as done for the solid profiles in Fig. 5.

longer pulse length chosen to limit the gradient strength. Although $E$ shows the expected increase for smaller $d$ there is a considerable deviation from the $1/d$ behaviour of the ideal case as given by Eq. (5). For larger $d$ there is additional signal increase due to repeated saturation, for smaller $d$ the enhancement is lower due to a suboptimal

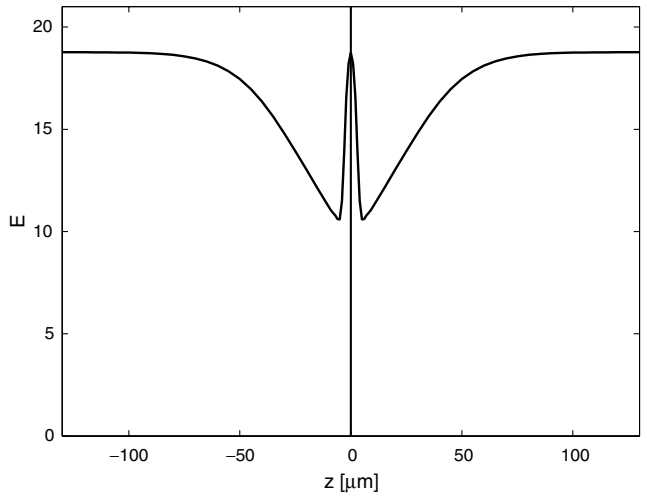


Fig. 7. Simulated DESIRE enhancement around a thin impermeable barrier with magnetisation excited on both sides of the barrier. The saturation pulse was moved in steps of $d/5$ to resolve the transition creating the peak around the barrier. See Fig. 5 for the used parameters and for example profiles depicted with dashed lines.

efficiency in exploiting the replaced spins with the chosen pulse repetition time. A similarly good agreement of experimental and simulated data shows Fig. 10 with $E$ determined as a function of the total saturation duration $T$ for two different resolutions. For $d = 5$ µm and $T = 10$ s a maximum value of $E = 25$ could be realised.

Finally, a 1D DESIRE image of the bottom edge in a Shigemi tube was acquired by moving the saturation of $d = 10$ µm in steps of 10 µm. Fig. 11 shows the resulting image with a maximum enhancement of $E = 11$. As expected the edge is not represented as a sharp step but as a smooth transition of the signal intensity. However, although the intensity initially follows the simulated values, there is no sudden signal drop right at the assumed location of the barrier. However, also in standard gradient echo imaging the edge is represented by a smooth signal decrease over about 80 µm, which is clearly beyond the width of the PSF including diffusion. Therefore we address this effect to a misalignment of about 1° between the gradient axis and the barrier surface in the Shigemi tube.

## 5. Discussion

A detailed experimental investigation was presented of the predictions given in Ref. [6] about the signal enhancement to be expected with 1D DESIRE, confirming the potential of the technique to dramatically increase the SNR in NMR microscopy. Simulations of a real implementation of the method proofed being a useful tool to elucidate the mechanisms of DESIRE saturation and to select experimental parameters. This was confirmed by the good quantitative agreement of simulated and measured results. Furthermore the contrast to be expected for DESIRE images taken from structured objects was investigated

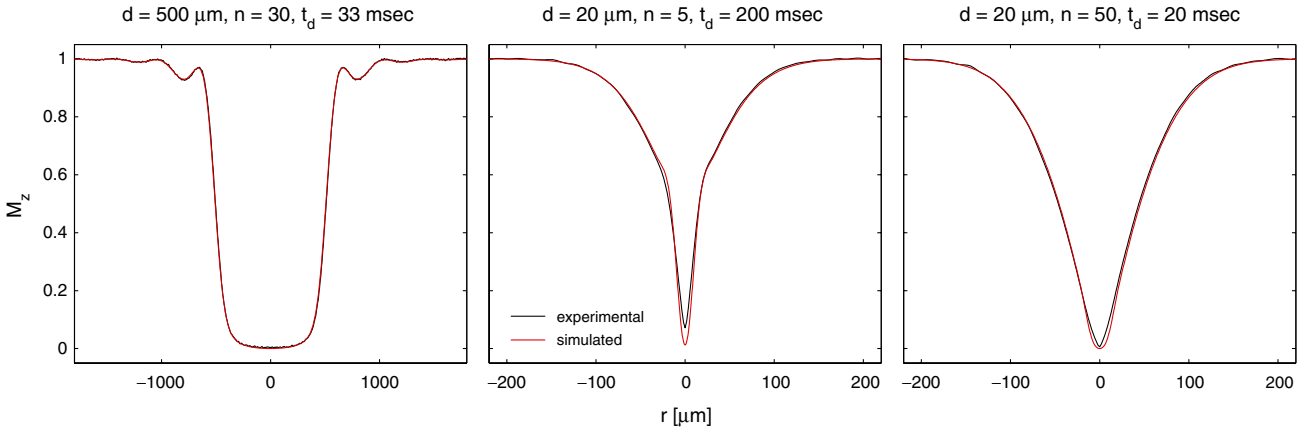


Fig. 8. Three examples of magnetisation profiles obtained by DESIRE saturation employing the indicated parameters. The profiles measured with the sequence depicted in Fig. 1b (black) show a good agreement with the corresponding simulated data (red).

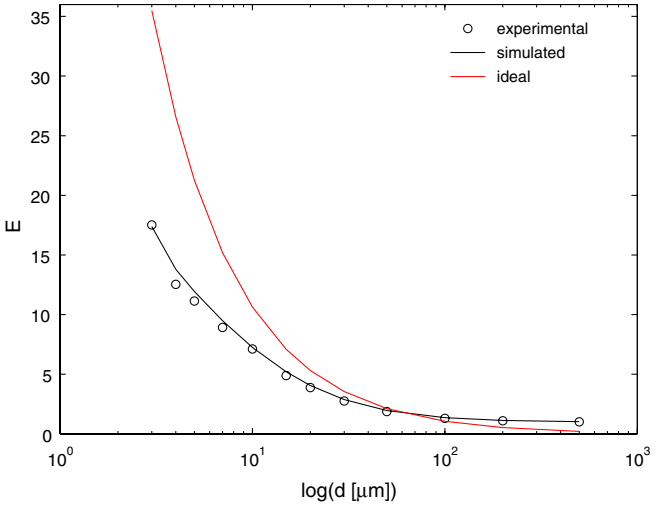


Fig. 9. Measured DESIRE enhancement as a function of the spatial resolution $d$. A series of 30 sinc-shaped saturation pulses was applied with $t_d = 33$ ms and $t_p = 3$ ms (5 ms for $d = 3$ µm). Simulated and experimental data show a reasonably good agreement whereas a considerable deviation from the $1/d$ dependence of the ideal case (see Eq. (5)) can be observed.

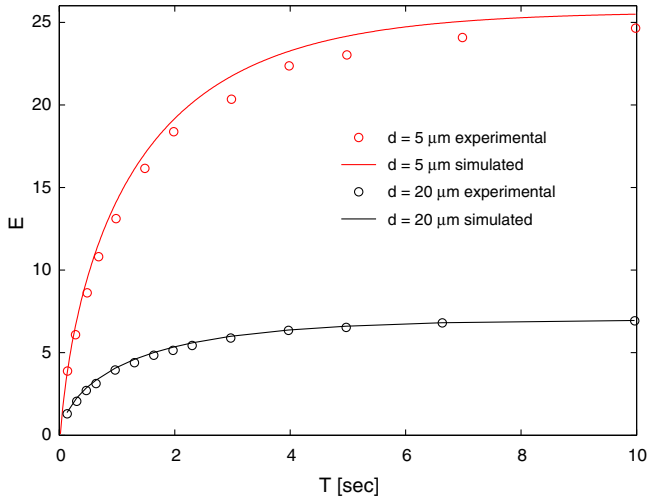


Fig. 10. Measured DESIRE enhancement as a function of the saturation duration $T$. For $d = 5$ and 20 µm series of up to 500 and 300 sinc-shaped saturation pulses were applied with $t_d = 20$ and 33 ms and $t_p = 3$ ms. Beside some minor deviations for $d = 5$ µm the experimental data agrees well with the simulated results, thus reflecting the asymptotic behaviour for the larger values of $T$.

and the first DESIRE image actually resolving a structural feature was presented.

Moving away from the ideal situation of a continuous source of saturated spins towards a practical implementation of a continuous saturation pulse or a series of pulses has a strong impact on the spatial resolution. The generally imperfect excitation profiles of finite pulses and the limited and locally different exchange of spins by diffusion lead to a local weighting that can be described by an effective saturation profile. In this work, the latter was used to derive measures for the effective spatial resolution of a certain setting. Considering these criteria the simulations revealed that the saturation parameters can be chosen in a way to provide both sufficient enhancement as well as effective resolution. However, it was also demonstrated that the effective resolution is a function of $D$ and thus can vary locally in a sample. However, this behaviour is not unique to DESIRE. Also in Fourier imaging the width of the $k$-space filter caused by diffusion depends on $D$ and therefore true resolution is a local property. Hence, for DESIRE more diffusion means not only more signal but also better resolution, whereas with Fourier techniques diffusion hampers both SNR and resolution.

Simulated and experimental results of DESIRE imaging confirmed earlier suggestions [6,7] that the signal intensity at a saturated location is strongly affected by nearby barriers. Hence, the signal obtained for this location does not only depend on the diffusion at the directly saturated location but also on structural and relaxation properties of the surrounding area within reach of the saturated spins. In the sense of what is usually expected from an imaging procedure one could conclude that the actually obtained resolu-

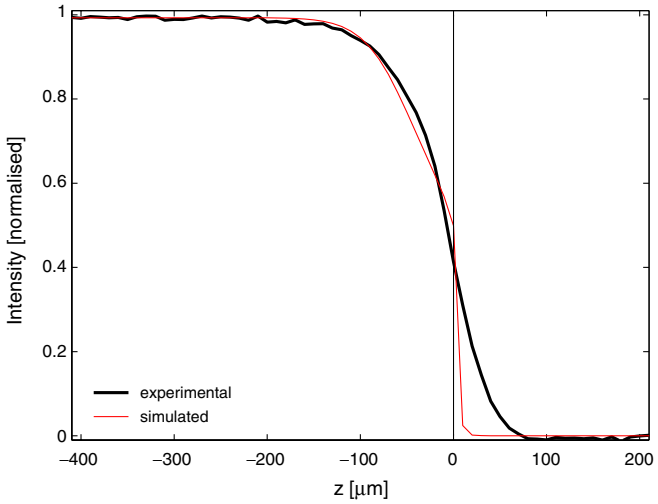


Fig. 11. 1D DESIRE imaging of the bottom edge in a Shigemi tube. Hundred sinc-shaped saturation pulses were applied with $d = 10$ μm, $t_d = 33$ ms, and $t_p = 3$ ms, providing a maximum signal enhancement of $E = 11$. The data for each sample were acquired by moving the position of the saturation in steps of 10 μm. As expected the signal intensity decreases when the barrier is approached. However, different from the simulated profile there is no sudden signal drop at the assumed barrier location. This effect is addressed to a slight angular misalignment between gradient axis and barrier surface.

tion is greatly reduced, thus fundamentally questioning the method. On the other hand, although DESIRE may not provide a direct spatial mapping, it still delivers useful structural information that only requires an appropriate interpretation. For example, signal intensity and shape in a closed compartment contain information about the size of and the diffusivity inside the compartment. Furthermore, as also discussed in Ref. [6] and simulated in this work, even narrow diffusion barriers that could never be resolved by conventional NMR imaging cause a characteristic signal variation in the nearby pixels. Similar effects of "edge enhancement" were also shown for Fourier imaging [11,12] but with a signal increase and shift, and without the general enhancement provided by DESIRE. Is has to be mentioned that in this work susceptibility effects were not taken into account but will also have a notable influence on the signal near barriers. Moreover, depending on the biological system to be imaged semi-permeable barriers [11] have to be assumed for an appropriate modelling of the expected image contrast.

Concerning practical implementations of DESIRE one has to be aware that a few aspects may hamper the realisation of the full gain in SNR efficiency. Being a saturation technique, the repetition time of the experiment must allow for full recovery of the magnetisation. Circumventing this problem by imaging separate regions in parallel (as suggested in Ref. [6]) or in an interleaved manner seems reasonable. However, the region size must be larger than the expected diffusion length, and the visible part of a sample will probably not contain many regions of such size. Furthermore, an analysis of the SNR efficiency must also account for the duration of the saturation period itself. On the other hand, it is an advantage of DESIRE that the field of view or even the voxels of interest can be freely chosen. The full SNR per voxel is directly available after a single shot, thus making the method very flexible. For example, regions of specific interest can be localised using a coarse sampling grid followed by scanning selected areas with the same resolution but reduced step-size, creating even a sub-resolution as described in Fig. 7. However, connected to this feature of a real-space imaging method is also the fact that temporal signal fluctuations of whatever origin directly enter the local image values.

Of course, real applications require 2D or 3D imaging, also providing much larger enhancement. As the DESIRE principle requires the localisation to be accomplished completely by the saturation pulse, more-dimensional excitation is required [13,14] which can become very long. It has been shown in the present study that the effective resolution is not obstructed by diffusion acting during the pulses. Hence, as usual the limitation to the pulse duration is given by the field inhomogeneities in the sample. Here, an approach that focuses only on the longitudinal magnetisation [15] or transmit SENSE [16] can help to keep the pulses sufficiently short.

In conclusion, the proven ability of 1D DESIRE to enhance signal in NMR microscopy, the prospects of up to three orders of magnitude signal gain for 3D imaging, and the associated time savings are intriguing. Moreover, unique structural information is expected from DESIRE images although their interpretation may be demanding. Therefore, although a few questions emerged concerning the practical implementation, it is still worthwhile continuing to explore the DESIRE approach. Expanding it to more dimensions and application to structured phantoms and cellular samples should give more insight into the true potential of the method.

## Acknowledgments

The authors thank Dieter Gross, Klaus Zick, and Thomas Oerther from Bruker Germany for technical advice. Andreas Trabesinger is acknowledged for important initial directions and Klaas Pruessmann for open-minded discussions. Furthermore we are grateful for the valuable comments of the reviewers of this manuscript.

## References

[1] L. Ciobanu, A.G. Webb, C.H. Pennington, Magnetic resonance imaging of biological cells, Prog. Nucl. Magn. Res. Spectrosc. 42 (2003) 69–93.
[2] P.T. Callaghan, C.D. Eccles, Diffusion-limited resolution in nuclear magnetic resonance microscopy, J. Magn. Reson. 78 (1988) 1–8.
[3] S. Gravina, D.G. Cory, Sensitivity and resolution of constant-time imaging, J. Magn. Reson. B 104 (1994) 53–61.
[4] M. Weiger, D. Schmidig, C. Massin, F. Vincent, S. Denoth, M. Schenkel, M. Fey, NMR microscopy with isotropic resolution down

to 3.0 μm using dedicated hardware, in: Proc. Intl. Soc. Mag. Reson. Med., Berlin, 2007, p. 3649.
[5] H.D. Morris, W.B. Hyslop, P.C. Lauterbur, Diffusion-enhanced NMR microscopy, in: Proc. Soc. Magn. Reson., San Francisco, 1994, p. 376.
[6] C.H. Pennington, Prospects for diffusion enhancement of signal and resolution in magnetic resonance microscopy, Concept Magn. Reson. 19A (2003) 71–79.
[7] L. Ciobanu, A.G. Webb, C.H. Pennington, Signal enhancement by diffusion: experimental observation of the "DESIRE" effect, J. Magn. Reson. 170 (2004) 252–256.
[8] H.C. Torrey, Bloch equations with diffusion terms, Phys. Rev. 104 (1956) 563–565.
[9] R.R. Ernst, G. Bodenhausen, A. Wokaun, Principles of Nuclear Magnetic Resonance in One and Two Dimensions, Clarendon Press, Oxford, 1991.
[10] K.R. Brownstein, C.E. Tarr, Importance of classical diffusion in NMR studies of water in biological cells, Phys. Rev. (1979) 2446–2453.
[11] W.B. Hyslop, P.C. Lauterbur, Effects of restricted diffusion on microscopic NMR imaging, J. Magn. Reson. 94 (1991) 501–510.
[12] B. Pütz, D. Barsky, K. Schulten, Edge enhancement by diffusion in microscopic magnetic resonance imaging, J. Magn. Reson. 97 (1992) 27–53.
[13] J. Pauly, D. Nishimura, A. Macovski, A *k*-space analysis of small-tip-angle excitation, J. Magn. Reson. 81 (1989) 43–56.
[14] J. Pauly, D. Nishimura, A. Macovski, A linear class of large-tip-angle selective excitation pulses, J. Magn. Reson. 82 (1989) 571–587.
[15] N. Yang, H.D. Morris, P.C. Lauterbur, Simple spatial localization of z-magnetization for DESIRE experiment, in: Proc. Soc. Magn. Reson., Nice, 1995, p. 1180.
[16] U. Katscher, P. Börnert, C. Leussler, J.S. van den Brink, Transmit SENSE, Magn. Reson. Med. 49 (2003) 144–150.